

# (Block) ILUT smoothers for $p$ -multigrid methods in Isogeometric Analysis

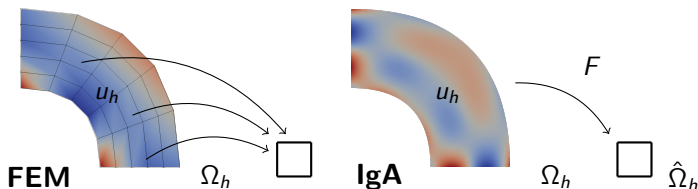
R. Tielen, M. Möller and C. Vuik

Delft University of Technology  
Delft Institute of Applied Mathematics

November 23, 2020

# Isogeometric Analysis (IgA)

- Extension of the Finite Element Method (FEM)
- Geometry  $\Omega$  and solution  $u$  are approximated by same basis functions (**B-Spline basis functions**)
- Global mapping from  $\Omega_h$  to parametric domain  $\hat{\Omega}_h$
- Description of the geometry that is highly accurate ( $'\Omega = \Omega_h'$ ) throughout all computation steps



## Model problem (CDR-equation)

Consider

$$-\nabla \cdot (D\nabla u) + v \cdot \nabla u + Ru = f, \quad \text{on } \Omega \quad (1)$$

$$u = g, \quad \text{on } \partial\Omega \quad (2)$$

where  $D$  denotes the diffusion tensor,  $v$  a divergence-free velocity field and  $R$  a source term. Here  $\Omega \subset \mathbb{R}^2$  is a connected, Lipschitz domain and  $f \in L^2(\Omega)$ .

Let  $\mathcal{V} = H_0^1(\Omega)$  denote the space of functions in the Sobolev space  $H^1(\Omega)$  that vanish at  $\partial\Omega$ .

# Variational formulation

Multiplication of Equation (1) with an arbitrary test function  $v \in \mathcal{V}$  and application of integration by parts leads to the variational form:

$$a(u, v) = (f, v) \quad \forall v \in \mathcal{V}, \quad (3)$$

where

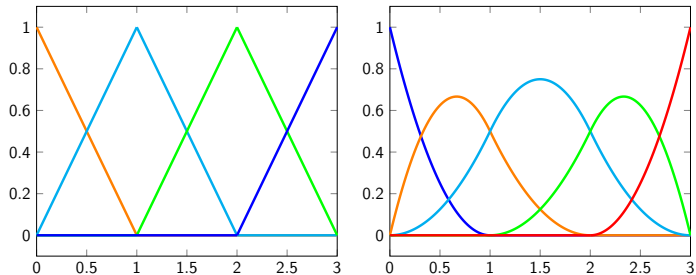
$$a(u, v) = \int_{\Omega} (D\nabla u) \cdot \nabla v + (v \cdot \nabla u)v + Ruv \, d\Omega$$

and

$$(f, v) = \int_{\Omega} fv \, d\Omega.$$

# B-spline basis functions

Isogeometric Analysis adopts **B-spline basis functions** to discretize the variational formulation

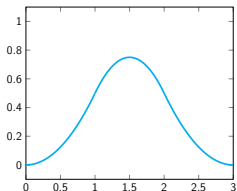
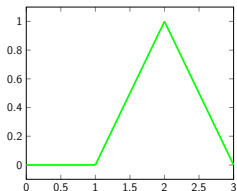
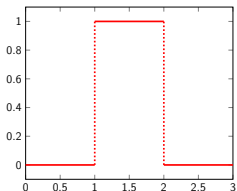


Linear ( $p = 1$ ) and quadratic ( $p = 2$ ) B-spline basis functions

# B-spline basis functions

## Properties of B-spline basis functions

- Compact support  $\Rightarrow$  Sparse system matrices
- Strictly positive  $\Rightarrow$  Mass matrix positive
- Partition of unity  $\Rightarrow$  Direct mass lumping



# Galerkin formulation

Given the spline space  $\mathcal{V}_{h,p}$ , the Galerkin formulation of (3) becomes:

Find  $u_{h,p} \in \mathcal{V}_{h,p}$  such that

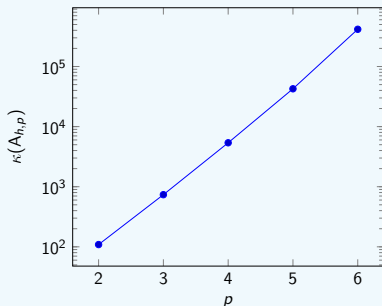
$$a(u_{h,p}, v_{h,p}) = (f, v_{h,p}) \quad \forall v_{h,p} \in \mathcal{V}_{h,p},$$

where  $p$  is the approximation order of the B-splines and  $h$  the mesh width. The discretized problem can be written as a linear system

$$A_{h,p} u_{h,p} = f_{h,p}. \quad (4)$$

## Need for efficient solvers

For a fixed mesh width  $h$ , the condition number  $\kappa(A_{h,p})$  scales exponentially with the approximation order  $p$ .



Standard (iterative) solvers become less efficient for higher values of  $p$ !

# Need for efficient solvers

## Enhanced $h$ -multigrid methods

- Subspace corrected mass smoother [Takacs, 2017]
- Hybrid smoother [Sogn, 2018]
- Multiplicative Schwarz smoother [de la Riva, 2018]

## Preconditioners

- Schwarz methods [Beirão da Veiga, 2012]
- Sylvester equation [Sangalli, 2016]

## **Our solution strategy:**

$p$ -multigrid methods [Tielen et al, 2018 & 2020]

## Motivation

The linear system  $A_{h,p}u_{h,p} = f_{h,p}$

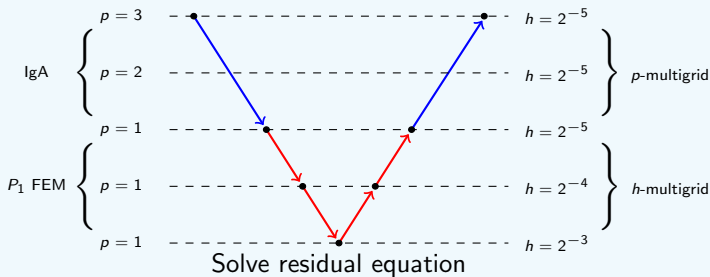
- ① becomes more difficult to solve for increasing  $p$
- ② reduces to standard  $C^0$ -FEM for  $p = 1$   
(where  $h$ -multigrid is an established solution technique)

In contrast to  $h$ -multigrid methods (in IgA)

- the #DoFs remains similar on coarser  $p$ -levels
- the stencil reduces significantly on coarse  $p$ -levels
- the spaces are not nested ( $\mathcal{V}_{h,p} \not\supset \mathcal{V}_{h,p-1} \not\supset \dots$ )

# $p$ -multigrid method

- Hierarchy of discretizations with different  $h$  and  $p$
- Low-order error is used to update high-order solution
- Smoothing step ( $\nu = 1$ ) is applied at each level (•)
- Gauss-Seidel as smoother on low-order level



# Prolongation and restriction

## Prolongation in $h$

$\mathcal{I}_{2h,1}^{h,1}$  is linear interpolation

## Restriction in $h$

$$\mathcal{I}_{h,1}^{2h,1} = \frac{1}{2} \left( \mathcal{I}_{2h,1}^{h,1} \right)^\top$$

## Prolongation in $p$

$$\mathcal{I}_{h,1}^{h,p} := (\mathbf{M}_p^p)^{-1} \mathbf{M}_1^p$$

## Restriction in $p$

$$\mathcal{I}_{h,p}^{h,1} := (\mathbf{M}_1^1)^{-1} \mathbf{M}_p^1$$

Let  $\phi_i^q$  denote the  $i^{\text{th}}$  basis function from  $\mathcal{V}_{h,q}$ . Then define

$$(\mathbf{M}_q^r)_{(i,j)} := \int_{\hat{\Omega}_h} \phi_i^q(\boldsymbol{\xi}) \phi_j^r(\boldsymbol{\xi}) c(\boldsymbol{\xi}) \, d\hat{\Omega}$$

Replace  $\mathbf{M}_q^q$  by its row-sum lumped counterpart!

## Smoother at high order level: Gauss-Seidel?

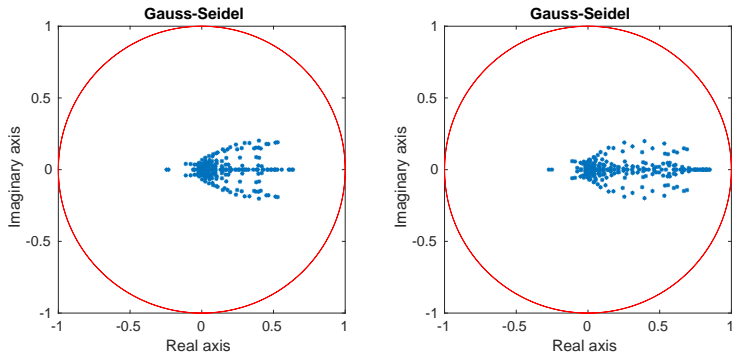


**Figure:** Spectrum iteration matrix  $p$ -multigrid for  $p = 2$  (left) and  $p = 3$  (right) for Poisson's equation on a quarter annulus.

## Alternative: ILUT smoother [Saad 1994]

**Setup:** Incomplete LU factorization of  $A_{h,p} \approx L_{h,p}U_{h,p}$  thereby

- 1 dropping all elements lower than tolerance  
 $\tau = 10^{-13}$
- 2 keeping only the  $N$  (= average number of non-zero entries in each row of  $A_{h,p}$ ) largest elements in each row

**Application:** perform  $s = 1, \dots, \nu$  smoothing steps

$$\begin{aligned}e_{h,p}^{(s)} &= (L_{h,p}U_{h,p})^{-1}(f_{h,p} - A_{h,p}u_{h,p}^{(s)}) \\u_{h,p}^{(s+1)} &= u_{h,p}^{(s)} + e_{h,p}^{(s)}\end{aligned}$$

# Spectrum iteration matrix ( $p=2$ )

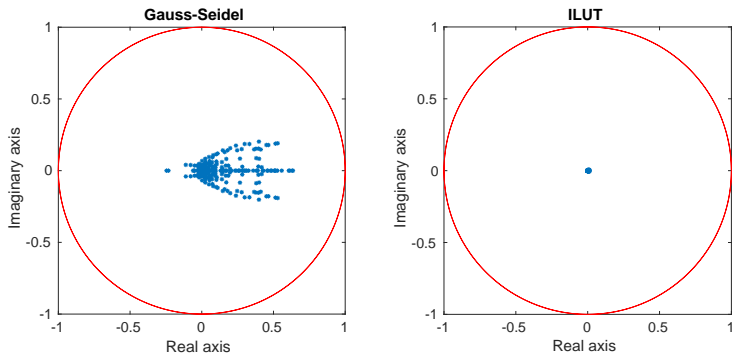


**Figure:** Spectrum iteration matrix for Gauss-Seidel (left) and ILUT (right) for Poisson's equation on a quarter annulus.

# Spectrum iteration matrix ( $p=3$ )

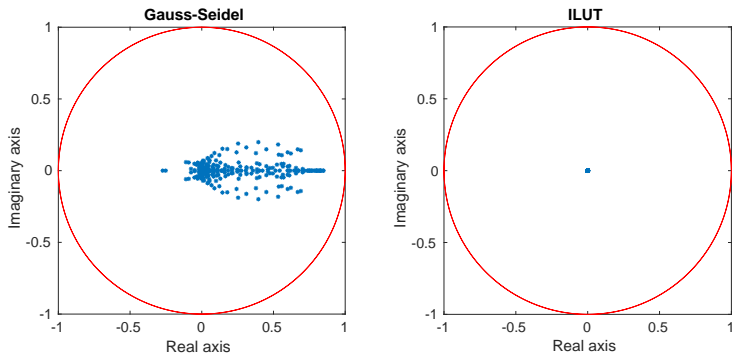


**Figure:** Spectrum iteration matrix for Gauss-Seidel (left) and ILUT (right) for Poisson's equation on a quarter annulus.

# Spectrum iteration matrix ( $p=4$ )

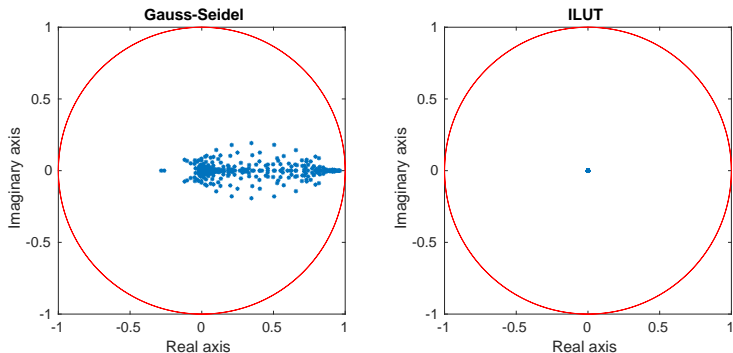


**Figure:** Spectrum iteration matrix for Gauss-Seidel (left) and ILUT (right) for Poisson's equation on a quarter annulus.

# Benchmark #1

- Poisson's equation:

$$D = \begin{bmatrix} 1 & 0 \\ 0 & 1 \end{bmatrix}, \quad v = \begin{bmatrix} 0 \\ 0 \end{bmatrix}, \quad R = 0.$$

- $\Omega$  is a quarter annulus with radii 1 and 2.

	$p = 2$		$p = 3$		$p = 4$		$p = 5$	
	ILUT	GS	ILUT	GS	ILUT	GS	ILUT	GS
$h = 2^{-6}$	4	30	3	62	3	176	3	491
$h = 2^{-7}$	4	29	3	61	3	172	3	499
$h = 2^{-8}$	5	30	3	60	3	163	3	473
$h = 2^{-9}$	5	32	3	61	3	163	3	452

## Benchmark #2

- CDR-equation:

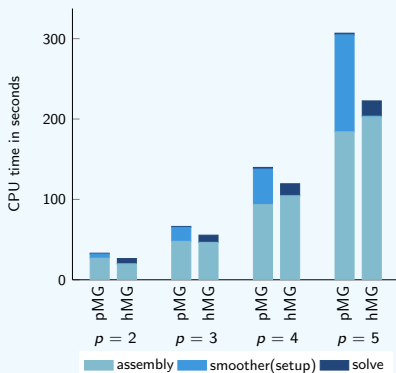
$$D = \begin{bmatrix} 1.2 & -0.7 \\ -0.4 & 0.9 \end{bmatrix}, \quad v = \begin{bmatrix} 0.4 \\ -0.2 \end{bmatrix}, \quad R = 0.3.$$

- $\Omega$  is the unit square, i.e.  $\Omega = [0, 1]^2$ .

	$p = 2$		$p = 3$		$p = 4$		$p = 5$	
	ILUT	GS	ILUT	GS	ILUT	GS	ILUT	GS
$h = 2^{-6}$	5	—	3	—	3	—	4	—
$h = 2^{-7}$	5	—	3	—	4	—	4	—
$h = 2^{-8}$	5	—	3	—	3	—	4	—
$h = 2^{-9}$	5	—	4	—	3	—	4	—

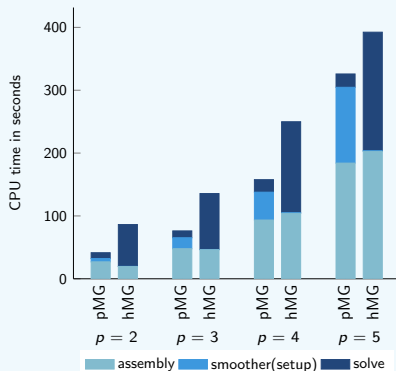
# CPU timings (single solve)

- Comparison with  $h$ -multigrid method [Takacs,2017]
- Higher setup costs with  $p$ -multigrid, but fast solves!



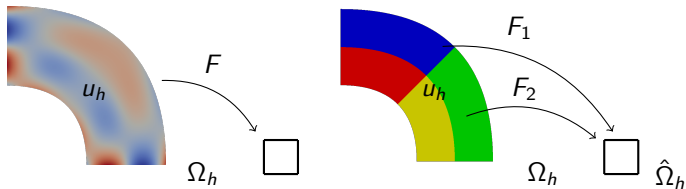
# CPU timings (Multiple solves)

- Typical example:  $Au_i = f_i$ ,  $i \in \{1, \dots, 10\}$
- Increasing influence of solving costs



# Multipatch geometries

- Geometry  $\Omega_h$  can **not always** be described by a single mapping to parametric domain  $\hat{\Omega}_h$ !
- Represent  $\Omega$  by non-overlapping subdomains (**patches**), each with their own mapping
- Resulting operator  $A_{h,p}$  has a block structure, where each patch leads to a single block



# Multipatch geometries

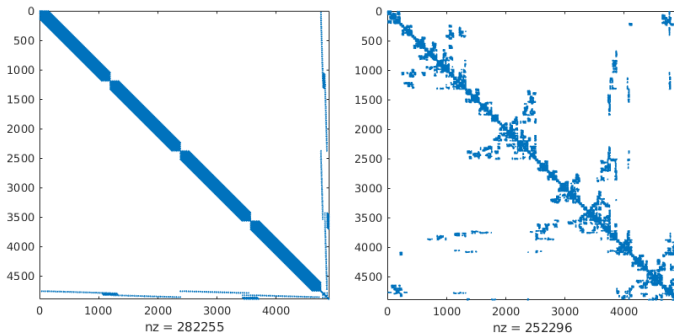


**Figure:** Sparsity pattern of the system matrix (left) and global ILUT factorization (right) for  $p = 3$  and  $h = 2^{-5}$  for Poisson's equation on a quarter annulus.

## Observation

We can write  $A = LU$  as:

$$\begin{bmatrix} A_{11} & & 0 & A_{\Gamma 1} \\ & \ddots & & \vdots \\ 0 & & A_{KK} & A_{\Gamma K} \\ A_{1\Gamma} & \cdots & A_{K\Gamma} & A_{\Gamma\Gamma} \end{bmatrix} = \begin{bmatrix} L_1 & & & \\ & \ddots & & \\ & & L_K & \\ B_1 & \cdots & B_K & I \end{bmatrix} \begin{bmatrix} U_1 & & & C_1 \\ & \ddots & & \vdots \\ & & U_K & C_K \\ & & & S \end{bmatrix},$$

where

- 1  $A_{ii} = L_i U_i$
- 2  $B_i = A_{i\Gamma} U_i^{-1}$
- 3  $C_i = L_i^{-1} A_{\Gamma i}$
- 4  $S = A_{\Gamma\Gamma} - \sum_{i=1}^K B_i C_i$

## Key Idea (Nievinski 2018)

Replace L and U by their ILUT factorizations:

$$\begin{bmatrix} A_{11} & & & A_{\Gamma 1} \\ & \ddots & & \vdots \\ A_{1\Gamma} & \cdots & A_{KK} & A_{\Gamma K} \\ & & A_{K\Gamma} & A_{\Gamma\Gamma} \end{bmatrix} \approx \begin{bmatrix} \tilde{L}_1 & & & \\ & \ddots & & \\ \tilde{B}_1 & \cdots & \tilde{B}_K & I \end{bmatrix} \begin{bmatrix} \tilde{U}_1 & & & \tilde{C}_1 \\ & \ddots & & \vdots \\ & & \tilde{U}_K & \tilde{C}_K \\ & & & \tilde{S} \end{bmatrix},$$

where

- 1  $A_{ii} \stackrel{(!)}{\approx} \tilde{L}_i \tilde{U}_i$
- 2  $\tilde{B}_i = A_{i\Gamma} \tilde{U}_i^{-1}$
- 3  $\tilde{C}_i = \tilde{L}_i^{-1} A_{\Gamma i}$
- 4  $\tilde{S} = A_{\Gamma\Gamma} - \sum_{i=1}^K \tilde{B}_i \tilde{C}_i$

# Block ILUT

- $\tilde{L}_i, \tilde{U}_i$  can be determined in parallel
- Inversion of  $\tilde{L}_i, \tilde{U}_i$  is avoided by solving:

$$U_i^T B_i^T = A_{i\Gamma}^T, \quad L_i C_i = A_{\Gamma i},$$

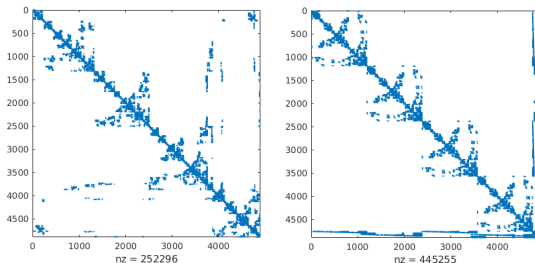


Figure: Global and block ILUT factorization for Poisson's equation

# Block ILUT vs. ILUT

## Poisson on Yeti Footprint

	$p = 2$		$p = 3$		$p = 4$		$p = 5$	
	Global	Block	Global	Block	Global	Block	Global	Block
$h = 2^{-3}$	5	4	4	2	4	2	4	2
$h = 2^{-4}$	8	4	5	3	5	3	4	2
$h = 2^{-5}$	8	4	6	3	5	3	5	3



## $p$ -multigrid methods

- 1 are efficient and robust solvers for IgA
- 2 enhanced with ILUT as a smoother they are
  - ▶ robust in the order  $p$  and mesh width  $h$
  - ▶ competitive to state-of-the-art  $h$ -multigrid methods
- 3 adopting block ILUT has potential (for parallelization) in case of multipatch geometries.

*$p$ -multigrid methods and their comparison to  $h$ -multigrid methods within Isogeometric Analysis, CMAME, 2020*



- Theoretical insight into effectiveness of ILUT
- Further exploration of block ILUT smoother
- Exploit parallelism of block ILUT smoother



G+Smo (Geometry plus Simulation modules),  
*<http://github.com/gismo>*